IEEE Photonics Journal
An IEEE Photonics Society Publication

High Extinction Ratio Magneto-Optical Fiber Modulator Based on Nanoparticle Magnetic Fluids

Volume 4, Number 4, August 2012

Peng Zu, Member, IEEE
Chi Chiu Chan, Member, IEEE
Wen Siang Lew
Yongxing Jin
Hwi Fen Liew
Li Han Chen
Wei Chang Wong
Xinyong Dong, Member, IEEE

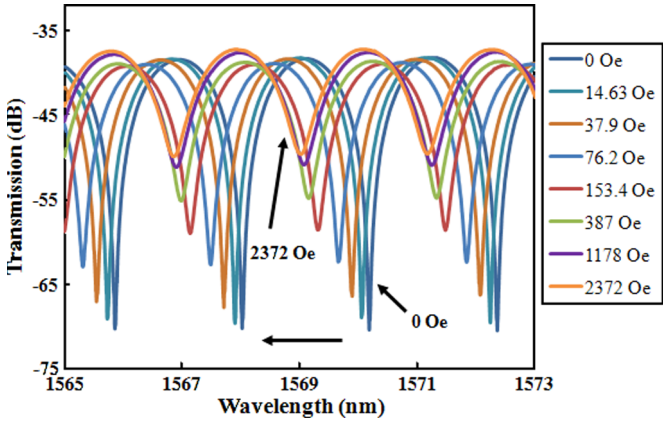

DOI: 10.1109/JPHOT.2012.2205233
1943-0655/$31.00 ©2012 IEEE

High Extinction Ratio Magneto-Optical Fiber Modulator Based on Nanoparticle Magnetic Fluids

Peng Zu,[1] *Member, IEEE*, Chi Chiu Chan,[1] *Member, IEEE*, Wen Siang Lew,[2] Yongxing Jin,[3] Hwi Fen Liew,[2] Li Han Chen,[1] Wei Chang Wong,[1] and Xinyong Dong,[3] *Member, IEEE*

[1]School of Chemical and Biomedical Engineering, Nanyang Technological University, Singapore 637459
[2]School of Physical & Mathematical Science, Nanyang Technological University, Singapore 637371
[3]Institute of Optoelectronic Technology, China Jiliang University, Hangzhou 310018, China

DOI: 10.1109/JPHOT.2012.2205233

Manuscript received April 14, 2012; revised June 14, 2012; accepted June 15, 2012. Date of publication June 19, 2012; date of current version July 2, 2012. Corresponding author: P. Zu (e-mail: xiaohaozi0716@hotmail.com).

Abstract: A novel magneto-optical fiber modulator with a high extinction ratio (ER) based on a polarization interference structure is proposed. A magnetic fluid (MF) film and a section of a polarization-maintaining fiber (PMF) are inserted into the structure to generate a suitable sinusoidal interference spectrum for light modulation. The MF film leads to a spectrum shift under external magnetic field due to its magnetically controllable birefringence, whereas the PMF is used to control the period of the interference spectrum. In this experiment, magneto-optical modulation with a high ER of 38 dB is demonstrated.

Index Terms: Magneto-optical modulator, magnetic fluid, extinction ratio.

1. Introduction

Magnetic fluid (MF) is a promising function material that possesses diverse attractive magneto-optical effects, including refractive index tunability, birefringence, dichroism, field-dependent transmission property, Faraday rotation, magnetochromatics, thermal–optical effects, and so on [1]–[7]. Taking advantage of these properties, a lot of MF-based photonics devices, especially optical fiber devices, were developed such as switches, modulators, magnetic field sensors, tunable filters, wavelength-division multiplexer (WDM), and so on [8]–[20]. Among these applications, magneto-optical modulators or switches were most intensively investigated and heavily reported [11]–[23], which can be further classified into two classes according to the modulation methods: intensity-modulation type and phase-modulation type. In intensity-modulation-type modulators, the light intensity is absorbed by the MF or attenuated by the MF-assisted fiber directly. The field-dependent transmission property of the MF is responsible for the absorption of the light, which was applied to realize light modulation with an extinction ratio (ER) of 0.8 dB [15]. ER is one of the most important parameters of the modulator, which is defined as the ratio of maximum to minimum of the optical transmission power when it is operated as ON- and OFF-state, respectively. Higher ER up to 10 dB can be achieved by increasing the thickness of the MF film at the cost of reducing modulation speed to hundreds of seconds [4]. Besides, MF-assisted fiber modulators were carried out by utilizing the MF as the refractive-index tunable cladding of an etched multimode fiber (MMF) [14] or a tampered single-mode fiber (SMF) [17] with ERs of 0.5–0.9 dB. The refractive index of the MF, which is

susceptible to temperature, should be carefully selected and controlled. In phase-modulation-type modulators, various optical interferometers are employed to convert the phase shift, which is induced by the magneto-optical effects of MF, to light intensity modulation indirectly. A Fabry–Perot interferometer (FPI) by utilizing the refractive index tunability of MF was reported as a tunable wavelength filter [10]. A fiber Mach–Zehnder interferometer (MZI) was demonstrated for optical signal processing with an ER of 0.55 dB [24]. A Sagnac interferometer (SI) with the MF film inserted into the fiber loop was also carried out to implement light intensity modulation with a greatly improved ER of 19.5 dB [13]. Most of current MF-based modulator applications are mainly based on its field-dependent transmission property or tunable refractive index. Birefringence is another important magneto-optical effect; however, few applications were reported. In this paper, a novel magneto-optical fiber modulator based on the birefringence property of MF is proposed, and its ER can be improved significantly.

2. Birefringence and Dichroism of the MF

The MF, which is also named as ferrofluid, is a highly stable magnetic colloidal suspension consisting of well-dispersed single-domain ferromagnetic nanoparticles in polar or nonpolar liquid carriers with the assistance of suitable surfactants [2]. The effective dielectric constant or refractive index of the MF is dependent on the dispersion state of the magnetic nanoparticles. Under zero magnetic field, the ferromagnetic nanoparticles disperse uniformly in the liquid carrier, and the MF as a whole exhibits homogeneity. If the MF is subjected to the external magnetic field, the homogenous state is broken, and the situation changes. The agglomeration occurs to the ferromagnetic nanoparticles in the liquid carrier, which leads to the phase separation between the nanoparticles and liquid carrier. Subsequently, the dielectric constant or refractive index of the MF is changed accordingly [22]. It has been shown that, the higher the external magnetic field strength, the more significant the phase separation and then the greater the variation of the magnetic field. Accompanied by the phase separation, the nanoparticles agglomerate and tend to form magnetic columns or magnetic chains along the direction of magnetic field to some extent; hence, the MF becomes an anisotropic structure under the external magnetic field. In this instance, the MF can be treated like a traditional optical crystal with optical axes. Since the magnetic columns or chains of ferromagnetic nanoparticles are aligned along the magnetic field direction, the slow axis of the MF is also aligned along the magnetic field direction, and, in turn, the fast axis of the MF is perpendicular to the magnetic field direction. The MF exhibits different refractive indices on the fast axis and slow axis. This phenomenon is referred to as the birefringence effect of the MF, which follows a Langevin function as the magnetic field strength is increased [3], [21]. If the light is launched into the MF perpendicularly to the magnetic field direction, then it will fall into two orthogonal polarized light beams, namely, the extraordinary light (e-ray, whose electric vector orients parallel to slow axis) and the ordinary light (o-ray, whose electric vector orients parallel to fast axis). The two orthogonal light beams travel with different propagation constants due to the birefringence effect, and a phase difference is accumulated over the thickness of the MF. Meanwhile, the e-ray and o-ray also experience different absorption coefficients in the MF due to the anisotropic structure, and this phenomenon is referred to as dichroism of the MF. Usually, the birefringence effect and the dichroism effect coexist in the MF under external magnetic field.

3. Structure and Operating Principle of the Magneto-Optical Modulator

The structure of the proposed modulator is shown in Fig. 1. The plane of the MF film is normal to the light propagating direction and parallel to the external magnetic field direction. The collimated light, which is linearly polarized after passing through the polarizer (P_1), is decomposed into two orthogonal linearly polarized beams when traveling in the MF film as well as the polarization-maintaining fiber (PMF). The e-ray and o-ray propagate at different speeds due to the birefringence effects of the MF film as well as the PMF and experience different absorption losses due to the dichroism effect of the MF film. Subsequently, the components of e-ray and o-ray on the direction of

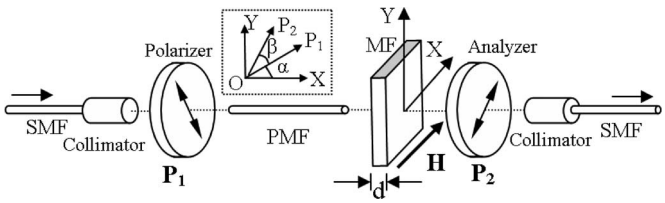

Fig. 1. Schematic diagram of the structure of the MF-based modulator.

the analyzer (P_2) interfere, and a wavelength-dependent polarization interference spectrum is produced at the analyzer (P_2).

In the configuration, the slow axis of the MF film (parallel to the magnetic field direction) is configured to be parallel to the fast axis of the PMF. So, the total phase difference is given as $\varphi = \varphi_{PM} - \varphi_{MF}$, where $\varphi_{PM} = 2\pi B_{PM} L/\lambda$ is the phase difference caused by the birefringence of PMF B_{PM} over the fiber length L, $\varphi_{MF} = 2\pi B_{MF} d/\lambda$ is the phase difference caused by the birefringence of MF film B_{MF} over the thickness of d, and λ is an operating wavelength. φ_{PM} is a constant, whereas φ_{MF} is a variable with the external magnetic field strength.

The linearly polarized light after P_1 is decomposed into two components along the slow axis and fast axis of the MF film, which can be given as: $E_0\cos\alpha$ and $E_0\sin\alpha$, respectively. E_0 is the amplitude of the electrical vector of the linear polarized light after P_1; α is the angle between P_1 direction and magnetic field direction X. After the MF film and the PMF, the two components become $E_0\cos\alpha \cdot e^{-\alpha_e d}$ and $E_0\sin\alpha \cdot e^{-\alpha_o d} e^{-i\varphi}$ for the X and Y direction, respectively. α_e and α_o are the according absorption coefficients for the two components, respectively. Subsequently, the two light components project on the P_2 direction again and become

$$E_1 = E_0\cos\alpha \cdot e^{-\alpha_e d} \cdot \cos(\alpha + \beta) \tag{1.1}$$

$$E_2 = E_0\sin\alpha \cdot e^{-\alpha_o d} e^{-i\varphi} \cdot \sin(\alpha + \beta) \tag{1.2}$$

where β is the angle between P_1 direction and P_2 direction. Then, the transmission function of the modulator $T = (E_1 + E_2) \cdot (E_1 + E_2)^*$ is deduced as

$$T = E_0^2 e^{-(\alpha_o+\alpha_e)d}\left[\cos^2\alpha\cos^2(\alpha+\beta)e^{-\Delta\alpha d} + \sin^2\alpha\sin^2(\alpha+\beta)e^{\Delta\alpha d} + 2\sin\alpha\cos\alpha\sin(\alpha+\beta)\cos(\alpha+\beta)\cos\varphi\right] \tag{2}$$

where $\Delta\alpha = \alpha_e - \alpha_o$ describes the dichroism property of MF. In the experiment, the analyzer P_2 is adjusted to be perpendicular to the polarizer P_1 (i.e., $\beta = 90°$); hence, (2) is simplified as

$$T = E_0^2 e^{-(\alpha_o+\alpha_e)d} \cdot \sin^2 2\alpha \cdot [\cosh(\Delta\alpha) - \cos\varphi]/2. \tag{3}$$

The transmission spectrum of the modulator is sinusoidal approximately (see Fig. 2). It is shown in Fig. 2 that ER of the modulator is equal to $\triangle$T. If the condition $\varphi = 2m\pi$ (m is an integer) is fulfilled, the transmission spectrum T is the minimum, and the transmission dips appear at the corresponding wavelengths on the transmission spectrum. The wavelength space between the two adjacent transmission dips S is given by

$$S = \lambda^2/(B_{PM}L - B_{MF}d). \tag{4}$$

A tunable laser with a narrow bandwidth is used to realize light modulation, and its wavelength is selected to be coincident with the dip wavelength of the interference spectrum under zero magnetic field (e.g., 1570.2 nm). It is shown in Fig. 2 that, without the external magnetic field, the transmission power reaches its minimum. As the external magnetic field is applied, the transmission spectrum shifts to the left, and the transmission power reaches its maximum. In order to obtain the light modulation with the best ER, the spectrum shift is expected to cover at least half period S of the spectrum.

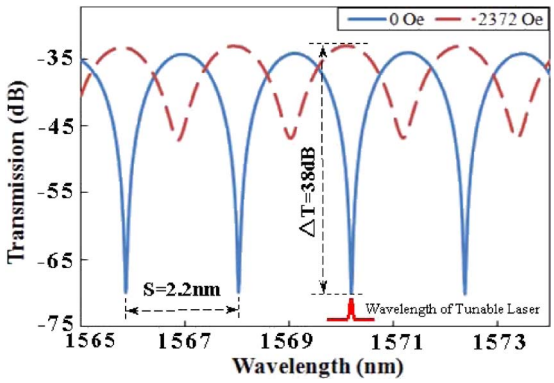

Fig. 2. Operating principle of the magneto-optical modulator based on the magnetically controllable transmission spectrum.

Compared with the length of PMF L, the thickness of MF film d (tens of micrometers) is so small that $B_{MF}d$ can be neglected, so S is mainly dependent on L. It is shown in (3) that the modulating ER is also affected by the visibility of the interference spectrum, which is determined by $e^{-(\alpha_o+\alpha_e)d}$ and $\sin^2 2\alpha$. In order to obtain the best visibility, α is set to be 45°. Finally, high modulating ER can be realized by selecting suitable length of PMF.

4. Experimental Results and Discussion

The water-based MF (EMG605, Ferrotec), whose content was 10-nm-diameter ferromagnetic nanoparticles, Fe_3O_4, was sealed between two 14 mm × 14 mm optical glass plates to form a 15-μm-thickness MF film. The concentration of the magnetic nanoparticles of the MF sample was 3.9%, and the MF film was light-brown translucent. The saturated magnetization and initial magnetic susceptibility of the MF used were 220 Oe and 2.96 Gs/Oe, respectively. The length of the PMF (PM-1550-HP) used in the experiment was 3 m, and its polarization extinction ratio (PER) was higher than 40 dB. The PERs of the polarizer and analyzer (Thorlabs) were both 40 dB. The central wavelength of the collimators was 1550 nm, and the beam diameter of the collimated light was about 0.5 mm. The MF film was placed amidst a uniform magnetic field, which was generated with an electromagnet (LakeShore) and calibrated with a gaussmeter (LakeShore). The dimension of the uniform region was about Φ65 mm × 25 mm, and the deviation of the uniformity was better than 0.05%. The magnetic field strength can be controlled by a personal computer. The experiment was conducted at the room temperature of 23.7 °C.

The transmission spectra of the magneto-optical modulator under different magnetic field strengths were measured with a broadband light source (1520–1610 nm) and an optical spectrum analyzer (OSA, AQ6370), which are shown in Figs. 2 and 3. The visibility of the transmission spectrum under zero magnetic field is about 36 dB, and the period is about 2.2 nm. As the magnetic field strength was increased from 0 Oe to 2372 Oe, the transmission spectrum shifted about 1.2 nm to the red side, as well as the visibility decreased from 36 dB to 13 dB, gradually. In order to investigate the variation trend of the transmission spectrum, the relationship between the dip wavelength (the third dip is chosen as an example) and the magnetic field strength is shown in Fig. 4(a). During the initial segment of the progression of magnetic field strength (e.g., $H < 200$ Oe), the dip wavelength varied quickly and linearly. As the magnetic field strength increases further, the shift of the dip wavelength becomes slow and nonlinear. As the magnetic field strength increased over a certain value (e.g., $H > 750$ Oe), the shift of the dip wavelength tended to be saturated. The curve for the decreasing process of the magnetic field strength was almost coincident with the one for the increasing process, which can be fitted well by modified Langevin function with a high goodness of fit R^2 value of 0.9982.

In order to verify the light intensity modulation property of the proposed modulator, a tunable laser (AQ8203) and a photodiode were applied to test the modulator. The wavelength of the tunable laser

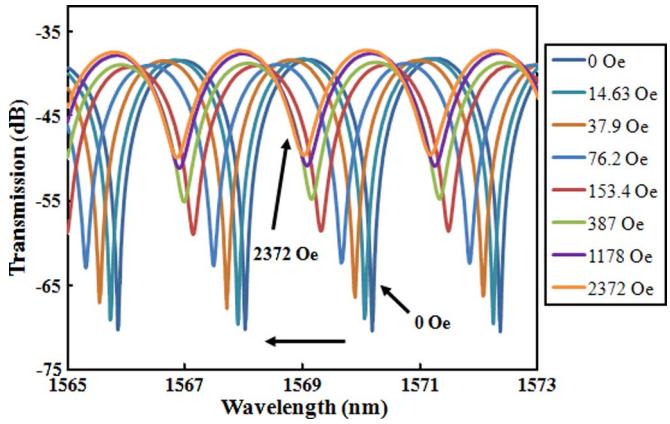

Fig. 3. Transmission spectra of the magneto-optical modulator under different applied magnetic field strengths.

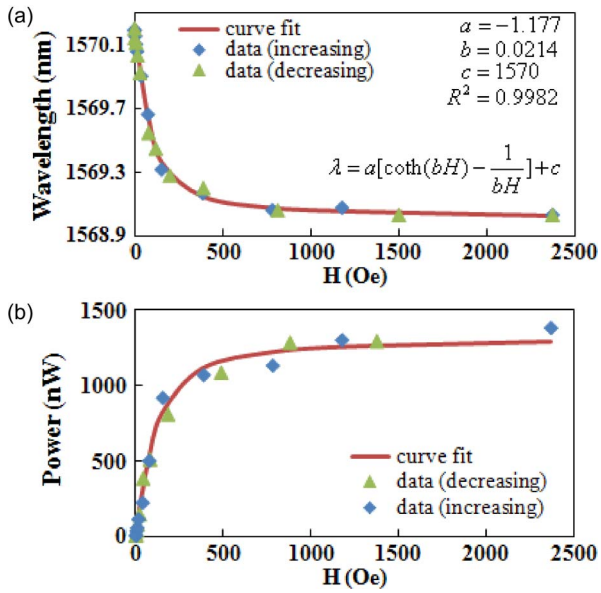

Fig. 4. (a) Dip wavelength and (b) transmission power versus the magnetic field strength.

was tuned to 1570.213 nm, which was coincident with the wavelength of the third dip on the transmission spectrum. The results are shown in Fig. 4(b). Similar to the variation trend of transmission spectrum, the light intensity varied quickly under small magnetic field strength and tended to be saturated under large magnetic field strength. The results in the processes of increasing and decreasing of the magnetic field strength are almost coincident, which show a good repeatability and indicate that hysteretic effect is absent in the MF. The curve is fitted with modified Langevin function with a R^2 value of 0.9912, which can be used to calibrate the nonlinearity between the light intensity and the magnetic field strength during the modulation.

The modulation characteristics of the proposed magneto-optical modulator are demonstrated by applying a square-wave and a sine-wave modulating magnetic fields on the MF film, and the corresponding light intensity modulation results are shown in Fig. 5. The magnetic field strengths for square-wave and sine-wave modulation were 1200 Oe and 100 Oe, whereas the corresponding ERs were about 38 dB and 29 dB, respectively. Limited by the speed of the magnetic field generation device, the waveform distortion appears. The frequency response of the modulator is

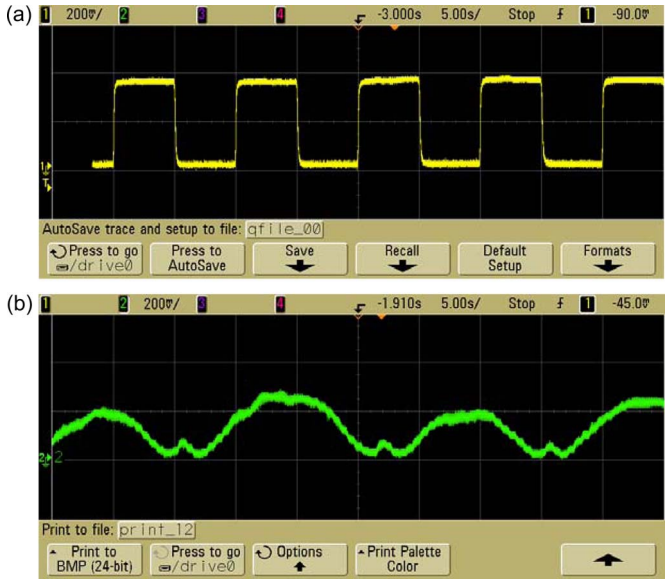

Fig. 5. Light intensity modulation by (a) square wave and (b) sine wave.

dependent on the response time of MF, which ranged from 10 ms to 600 ms [12], [19], [24]. Hence, the highest frequency of such modulator is about 100 Hz. The response time can further be improved by reducing concentration of the MF or by using other types of the magneto-optical material such as YIG [25], [26]. Due to the response time of MF, the modulator cannot work in high modulation frequency. However, it can be used to generate low-frequency control signal in the optical communication system. Also, it is good enough for applications such as switch, routers, and display.

5. Conclusion

In conclusion, the feasibility of the proposed magneto-optical modulator based on MF film is verified. The magnetically controllable birefringence property of MF plays a key role in the optical modulator. The light intensity was modulated into square wave and sine wave with high ERs of 38 dB and 29 dB, respectively. The PMF-assisted structure is very simple, which can be developed into an integrated fiber device, potentially.

References

[1] H. E. Horng, C. Y. Hong, S. Y. Yang, and H. C. Yang, "Designing the refractive indices by using magnetic fluids," *Appl. Phys. Lett.*, vol. 82, no. 15, pp. 2434–2436, Apr. 2003.
[2] Z. Y. Di, X. F. Chen, S. L. Pu, X. Hu, and Y. X. Xia, "Magnetic-field-induced birefringence and particle agglomeration in magnetic fluids," *Appl. Phys. Lett.*, vol. 89, no. 21, pp. 211106-1–211106-3, Nov. 2006.
[3] M. Xu and P. J. Ridler, "Linear dichroism and birefringence effects in magnetic fluids," *J. Appl. Phys.*, vol. 82, no. 1, pp. 326–332, Jul. 1997.
[4] J. Li, X. D. Liu, Y. Q. Lin, L. Bai, Q. Li, X. M. Chen, and A. R. Wang, "Field modulation of light transmission through ferrofluid film," *Appl. Phys. Lett.*, vol. 91, no. 25, pp. 253108-1–253108-3, Dec. 2007.
[5] Y. T. Pan, C. W. Du, X. D. Liu, Z. G. Li, and R. Birngruber, "Wavelength dependence of the Faraday-effect and magnetobirefringence in ferrofluid thin-films," *J. Appl. Phys.*, vol. 73, no. 10, pp. 6139–6141, May 1993.
[6] S. L. Pu, X. F. Chen, W. J. Liao, L. J. Chen, Y. P. Chen, and Y. X. Xia, "Laser self-induced thermo-optical effects in a magnetic fluid," *J. Appl. Phys.*, vol. 96, no. 10, pp. 5930–5932, Nov. 2004.
[7] H. E. Horng, S. Y. Yang, S. L. Lee, C. Y. Hong, and H. C. Yang, "Magnetochromatics of the magnetic fluid film under a dynamic magnetic field," *Appl. Phys. Lett.*, vol. 79, no. 3, pp. 350–352, Jul. 2001.
[8] T. Liu, X. Chen, Z. Di, J. Zhang, X. Li, and J. Chen, "Tunable magneto-optical wavelength filter of long-period fiber grating with magnetic fluids," *Appl. Phys. Lett.*, vol. 91, no. 12, pp. 121116-1–121116-3, Sep. 2007.
[9] Y. W. Huang, S. T. Hu, S. Y. Yang, and H. E. Horng, "Tunable diffraction of magnetic fluid films and its potential application in coarse wavelength-division multiplexing," *Opt. Lett.*, vol. 29, no. 16, pp. 1867–1869, Aug. 2004.

[10] T. Hu, Y. Zhao, X. Li, J. Chen, and Z. Lv, "Novel optical fiber current sensor based on magnetic fluid," *Chin. Opt. Lett.*, vol. 8, no. 4, pp. 392–394, Apr. 2010.
[11] H. E. Horng, C. S. Chen, K. L. Fang, S. Y. Yang, J. J. Chieh, C. Y. Hong, and H. C. Yang, "Tunable optical switch using magnetic fluids," *Appl. Phys. Lett.*, vol. 85, no. 23, pp. 5592–5594, Dec. 2004.
[12] S. L. Pu, X. F. Chen, Z. Y. Di, and Y. X. Xia, "Relaxation property of the magnetic-fluid-based fiber-optic evanescent field modulator," *J. Appl. Phys.*, vol. 101, no. 5, pp. 053532-1–053532-5, Mar. 2007.
[13] P. Zu, C. C. Chan, L. W. Siang, Y. X. Jin, Y. F. Zhang, L. H. Fen, L. H. Chen, and X. Y. Dong, "Magneto-optic fiber Sagnac modulator based on magnetic fluids," *Opt. Lett.*, vol. 36, no. 8, pp. 1425–1427, Apr. 2011.
[14] J. J. Chieh, S. Y. Yang, H. E. Horng, C. Y. Hong, and H. C. Yang, "Magnetic-fluid optical-fiber modulators via magnetic modulation," *Appl. Phys. Lett.*, vol. 90, no. 13, pp. 133505-1–133505-3, Mar. 2007.
[15] H. Horng, S. Yang, W. Tse, H. Yang, W. Luo, and C. Hong, "Magnetically modulated optical transmission of magnetic fluid films," *J. Magn. Magn. Mater.*, vol. 252, pp. 104–106, 2002.
[16] S. Y. Park, H. Handa, and A. Sandhu, "High speed magneto-optical valve: Rapid control of the optical transmittance of aqueous solutions by magnetically induced self-assembly of superparamagnetic particle chains," *J. Appl. Phys.*, vol. 105, no. 7, pp. 07B526–07B526, Apr. 2009.
[17] S. L. Pu, X. F. Chen, Y. P. Chen, Y. H. Xu, W. J. Liao, L. J. Chen, and Y. X. Xia, "Fiber-optic evanescent field modulator using a magnetic fluid as the cladding," *J. Appl. Phys.*, vol. 99, no. 9, pp. 093516-1–093516-4, May 2006.
[18] H. D. Deng, J. Liu, W. R. Zhao, W. Zhang, X. S. Lin, T. Sun, Q. F. Dai, L. J. Wu, S. Lan, and A. V. Gopal, "Enhancement of switching speed by laser-induced clustering of nanoparticles in magnetic fluids," *Appl. Phys. Lett.*, vol. 92, no. 23, pp. 233103-1–233103-3, Jun. 2008.
[19] J. J. Chieh, S. Y. Yang, Y. H. Chao, H. E. Horng, C. Y. Hong, and H. C. Yang, "Dynamic response of optical-fiber modulator by using magnetic fluid as a cladding layer," *J. Appl. Phys.*, vol. 97, no. 4, pp. 043104-1–043104-4, Feb. 2005.
[20] J. W. Seo, H. Kim, and S. Sung, "Design and fabrication of a magnetic microfluidic light modulator using magnetic fluid," *J. Magn. Magn. Mater.*, vol. 272, pp. E1787–E1789, May 2004.
[21] P. Zu, C. C. Chan, W. S. Lew, Y. Jin, Y. Zhang, H. F. Liew, L. H. Chen, W. C. Wong, and X. Dong, "Magneto-optical fiber sensor based on magnetic fluid," *Opt. Lett.*, vol. 37, no. 3, pp. 398–400, Feb. 2012.
[22] P. Zu, C. C. Chan, W. S. Lew, L. Hu, Y. Jin, H. F. Liew, L. H. Chen, W. C. Wong, and X. Dong, "Temperature-insensitive magnetic field sensor based on nanoparticle magnetic fluid and photonic crystal fiber," *IEEE Photon. J.*, vol. 4, no. 2, pp. 491–498, Apr. 2012.
[23] L. O'Faolain, D. M. Beggs, T. P. White, T. Kampfrath, K. Kuipers, and T. F. Krauss, "Compact optical switches and modulators based on dispersion engineered photonic crystals," *IEEE Photon. J.*, vol. 2, no. 3, pp. 404–414, Jun. 2010.
[24] J. Chieh, C. Hong, S. Yang, H. Horng, and H. Yang, "Study on magnetic fluid optical fiber devices for optical logic operations by characteristics of superparamagnetic nanoparticles and magnetic fluids," *J. Nanoparticle Res.*, vol. 12, no. 1, pp. 293–300, Jan. 2010.
[25] D. Hutchings and B. Holmes, "A waveguide polarization toolset design based on mode beating," *IEEE Photon. J.*, vol. 3, no. 3, pp. 450–461, Jun. 2011.
[26] M. Attygalle, K. Gupta, and T. Priest, "Broadband extended dynamic range analogue signal transmission through switched dual photonic link architecture," *IEEE Photon. J.*, vol. 3, no. 1, pp. 100–111, Feb. 2011.